Available online at www.sciencedirect.com
ScienceDirect
Earth and Planetary Science Letters 252 (2006) 308–326
EPSL
www.elsevier.com/locate/epsl

# How juvenile is the Arabian–Nubian Shield? Evidence from Nd isotopes and pre-Neoproterozoic inherited zircon in the Bi'r Umq suture zone, Saudi Arabia

U.S. Hargrove [a,*], R.J. Stern [a], J.-I. Kimura [b], W.I. Manton [a], P.R. Johnson [c]

[a] *Department of Geosciences, University of Texas at Dallas, Box 830688, Richardson, TX 75083-0688, USA*
[b] *Department of Geoscience, Shimane University, Matsue City 690-8504, Japan*
[c] *Saudi Geological Survey, Box 54141, Jeddah 21514, Saudi Arabia*

Received 24 September 2005; received in revised form 30 September 2006; accepted 1 October 2006
Available online 7 November 2006
Editor: R.W. Carlson

**Abstract**

The Bi'r Umq suture zone (BUSZ) in western Saudi Arabia comprises Neoproterozoic oceanic-arc plutonic, volcanosedimentary, and ophiolitic rocks that record some of the earliest magmatic and tectonic events of the East African Orogen in the Arabian–Nubian Shield (ANS). New Nd isotopic analyses are combined with data on zircon inheritance and published isotopic studies to establish the case that pre-Neoproterozoic crust had a greater influence on the oceanic portion of the ANS than is appreciated.

Highly positive initial εNd (+3.9 to +8.5) and Nd model ages (560–830 Ma) that approximate crystallization ages (573–813 Ma) of BUSZ igneous rocks are comparable to upper crust in other parts of the ANS considered to be juvenile (mantle-derived) and to some xenoliths from the lower crust and lithospheric mantle. Overall, the data suggest that the 40-km-thick crust beneath much of the Arabian Shield is juvenile and that most of it was extracted from depleted mantle during the interval ~740–830 Ma.

Although much of the ANS is isotopically juvenile, some Neoproterozoic igneous rocks in the northern ANS contain zircon inherited from pre-Neoproterozoic sources. Samples from the BUSZ that show inheritance yield slightly lower initial εNd than contemporary samples that do not show inheritance, suggesting that some juvenile magmas assimilated older continental material. The age of that material is inferred to be largely early Neoproterozoic and Mesoproterozoic, with minor Paleoproterozoic and Archean components, based on U–Pb ages of inherited zircon and Nd model ages for ANS upper crustal rocks and xenoliths of the lower crust and mantle lithosphere.

Inherited zircon may have been assimilated from terrigenous sediment shed from nearby passive margins, and transported fluvially or by glaciers, or by assimilation of cryptic early Neoproterozoic to Archean basement that underlies the "juvenile" core of the ANS. Zircon morphologies are consistent with both sedimentary origins and in situ extraction from older basement, although inheritance in the Tharwah ophiolite argues for the latter (i.e. during rifting of pre-existing arc crust). Assuming a sedimentary origin, Paleoproterozoic–Archean inherited zircon may be derived from basement of that age exposed in the ANS, but Mesoproterozoic sources do not occur anywhere in the shield.


*Keywords:* Arabian–Nubian Shield; East African Orogen; Neoproterozoic; Nd isotopes; U–Pb zircon; inheritance

* Corresponding author. Present address: ADEXCO Production Co., 309 W. 7th St., Ste. 400, Ft. Worth, TX 76102, USA. Tel.: +1 817 332 3891; fax: +1 817 332 3894.
*E-mail address:* trey@adexco.net (U.S. Hargrove).

0012-821X/$ - see front matter © 2006 Elsevier B.V. All rights reserved.
doi:10.1016/j.epsl.2006.10.002

## 1. Introduction

The origins and evolution of continental crust are among the great outstanding problems in solid Earth systems research. It is widely accepted that most modern juvenile continental crust (i.e. crust formed directly from the mantle) is produced at convergent plate margins [1]. However, controversy persists on several important points, in particular the rates at which juvenile crust is formed and the importance of the extraction of juvenile continental crust from the mantle vs. the recycling of pre-existing crust [2]. Here we contribute to the resolution of this controversy by using the different perspectives gained from U–Pb zircon dating and Nd isotopic studies of igneous rocks in a portion of the Arabian–Nubian Shield (ANS), a region of Precambrian basement in Arabia and northeast Africa (Fig. 1) exposed as a result of rifting along the Red Sea. The ANS is an outstanding natural laboratory for studying the origin and evolution of juvenile continental crust: it arguably contains the best-preserved and most widely exposed ($>6\times10^6$ km$^2$) juvenile continental crust of

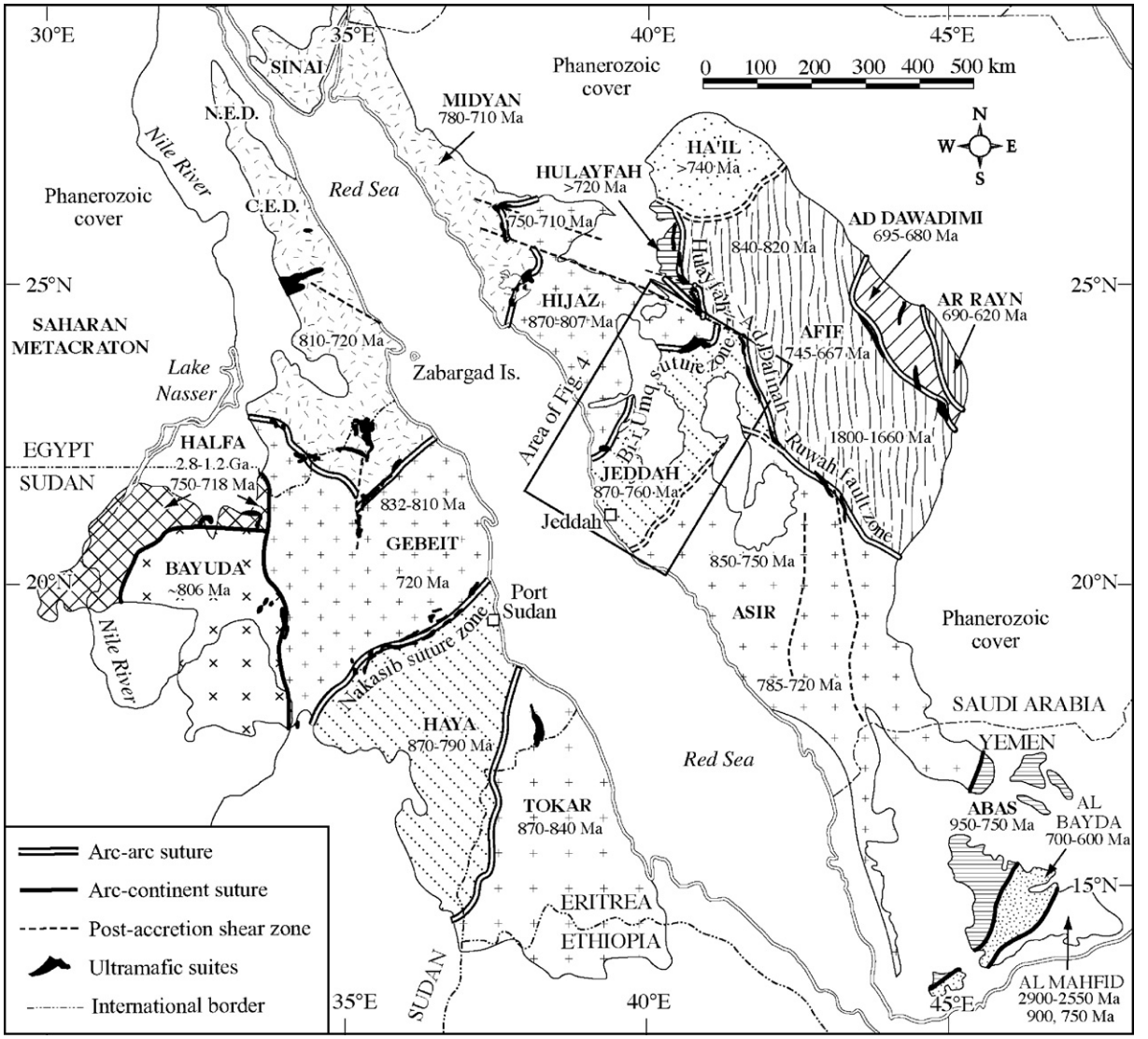


Fig. 1. Tectonic map of the Arabian–Nubian Shield, modified after Johnson and Woldehaimanot [14], showing the distribution of tectonomagmatic terranes, sutures, and mafic–ultramafic (ophiolite) suites. Ages indicated are for terrane protoliths. Data sources include Agar et al. [65], Windley et al. [66], Whitehouse et al. [16,19,67], and references in Johnson and Woldehaimanot [14]. Similar patterns indicate correlation of terranes across the Red Sea. The location of Fig. 4 is outlined. N.E.D., Northern Eastern Desert; C.E.D., Central Eastern Desert.

Neoproterozoic age (1000 to 542 Ma; [3]) on the planet [4–7]; it has the thickness (~40 km) of true continental crust [8] and a P-wave velocity structure typical of continental crust generated since the Archean [9]; and samples of the deep ANS crust and mantle lithosphere exhumed by Tertiary basalts are compositionally like those expected for continental lithosphere formed from juvenile crust in Neoproterozoic time [10–12].

Much, but not all, of the ANS formed in Neoproterozoic time by processes indistinguishable from those of modern plate tectonics, as it is a collage of well-defined intra-oceanic tectonostratigraphic arc terranes, which are separated by identifiable sutures commonly marked by ophiolites [13,14]. It is generally agreed that most of the ANS consists of juvenile Neoproterozoic crust (Fig. 2). However, geological (e.g., [15]), geochronological (e.g.,

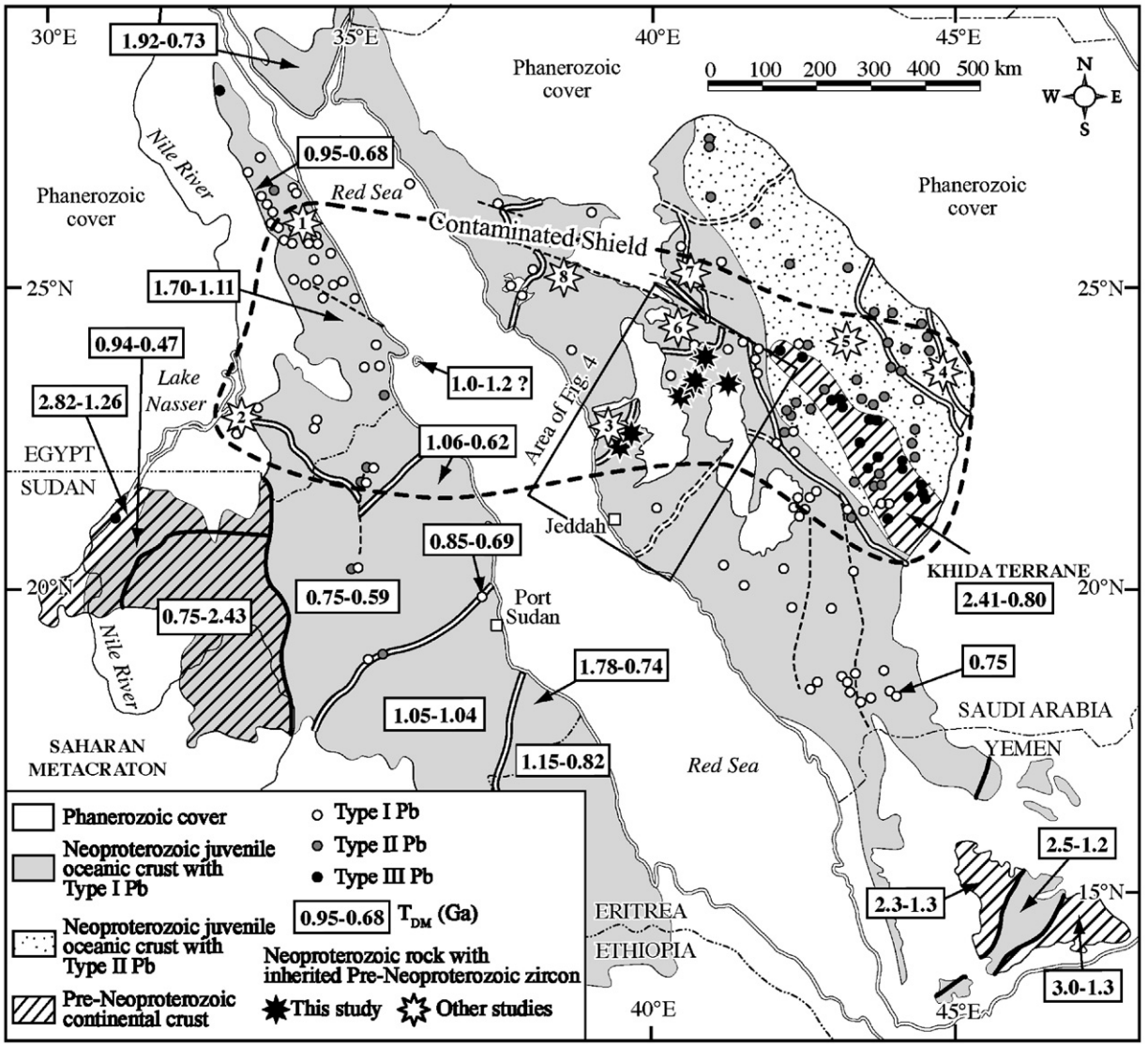


Fig. 2. Map of the Arabian–Nubian Shield, modified after Johnson and Woldehaimanot [14], showing the locations of Pb and Nd isotopic samples and the locations of samples from this (filled stars) and other studies (open stars labelled 1–8) that contain zircon inherited from pre-Neoproterozoic sources. Bold dashed line encloses the approximate extent of the shield contaminated by pre-Neoproterozoic crust or sediment derived therefrom, as presently understood. Data for zircon inheritance are from [23–27,29,30]. The division of the shield into oceanic, intermediate, and continental crust types is based on initial Pb and Nd isotopic data from (references in [14,18,22,24–26,30,57,58,66–71]). Lead isotope classification is that of Stoeser and Stacey [32]: Type I reflects primitive (oceanic) lead; Type II is primitive lead contaminated by more evolved lead; and Type III is evolved (continental) lead. $\varepsilon_{Nd}(T)$=initial epsilon Nd; $T_{DM}$=Nd model ages, based on model of DePaolo [37]. The location of Fig. 4 is outlined.

[16]), and Pb, Nd, and Sr isotopic data (e.g., [17–19]) indicate that the central parts of the Afif terrane, commonly referred to as the Khida terrane, in Saudi Arabia and parts of the shield in Yemen (Figs. 1 and 2) are underlain or were influenced by Paleoproterozoic (1600–2500 Ma) to Archean (>2500 Ma) continental crust. Crust of similar age is also exposed in the Saharan Metacraton [20] at the western margin of the Halfa terrane in Sudan (Figs. 1 and 2) (e.g., [21,22]). Exposures of pre-Neoproterozoic continental crust in those areas exhibit evolved initial $^{207}Pb/^{206}Pb$, commonly negative initial epsilon Nd ($\varepsilon_{Nd}(T)$), and Nd model ages ($T_{DM}$) that significantly predate crystallization ages (Fig. 2), as expected for evolved continental crust. The juvenile core of the ANS, comprising the Gerf–Midyan, Gebeit–Hijaz, Haya–Jeddah, Asir–Tokar, and Hulayfah terranes as well as the westernmost parts of the Afif and Ha'il terranes, is characterized by primitive initial $^{207}Pb/^{206}Pb$, highly positive $\varepsilon_{Nd}(T)$, and $T_{DM}$ ages that approximate crystallization ages (Figs. 1 and 2) ([14], and references therein), as expected for intra-oceanic arc crust. Remaining parts of the shield exhibit isotopic signatures of oceanic crust contaminated by continental material (Fig. 2). The reader is referred to Johnson and Woldehaimanot [14] for a more thorough overview of the ANS and its geological history.

The extent of the juvenile ANS affected by pre-Neoproterozoic crust, which is referred to herein as the "contaminated shield," is poorly constrained and is probably greater than that shown in Fig. 2. Although isotopic data indicate that older crust had little influence on the juvenile core of the ANS, U–Pb zircon studies there have documented inheritance (assimilation of xenocrystic zircon by magma); localities showing inheritance are indicated in Fig. 2. Indirect evidence for pre-Neoproterozoic inheritance in the "juvenile" ANS comes from the Central Eastern Desert of Egypt (Fig. 1; locality 1 in Fig. 2), where post-tectonic granite yielded a conventional $^{207}Pb/^{206}Pb$ zircon age of 578±15 Ma, based on one nearly concordant analysis, but contained an older component with a maximum age of ~1650 Ma [23]. The granite also yielded high initial $^{87}Sr/^{86}Sr$ and $^{207}Pb/^{204}Pb$ compared to more primitive rocks of the same age from the shield, despite initial $\varepsilon_{Nd}$ (+5.7) typical of juvenile crust [23].

More direct evidence comes from studies of Neoproterozoic ophiolites in the ANS. A felsic dike intruding the Wadi Allaqi ophiolite in eastern Egypt (locality 2 in Fig. 2) yielded a conventional $^{207}Pb/^{206}Pb$ zircon age of 770 Ma (the minimum age for the ophiolite), but xenocrystic zircon yielded an age of 3017 Ma, which was interpreted as evidence that Archean basement, probably part of the Saharan Metacraton, occurs beneath that part of the juvenile shield [24]. In another example, Pallister et al. [25] obtained a nearly concordant, conventional zircon model age of 870±11 Ma for gabbro in the Tharwah ophiolite along the Bi'r Umq suture zone in western Saudi Arabia (locality 3 in Fig. 2). Two xenocrystic zircon fractions yielded highly discordant model ages of ~1250 Ma, which were interpreted to reflect assimilation of older (>1250 Ma) material during emplacement of the gabbroic magma. Hargrove et al. [26] and Hargrove [27] dated zircon from the same gabbro in the Tharwah ophiolite by ion microprobe, which has the advantage over conventional techniques of being able to analyze multiple parts of a single grain and discriminate between juvenile and inherited zircon. They obtained a two-point concordia age (after the terminology of [28]) of 777±17 Ma for a juvenile zircon fraction and interpreted the ~1130 Ma concordia age of another fraction to indicate inheritance from a Mesoproterozoic source. Those authors further suggested that the 777 Ma age is a better approximation of the igneous age of the ophiolite and that the 870 Ma age obtained by Pallister et al. [25] is most likely a composite of the igneous age of the ophiolite and the age of a Mesoproterozoic contaminant. This is a particular problem because crust of Mesoproterozoic age is not exposed anywhere in the vicinity of the ANS.

Additional direct evidence of pre-Neoproterozoic inheritance has also been found in non-ophiolitic Neoproterozoic rocks in Arabia. Gabbroic-trondhjemitic rocks in the Al Amar suture zone (locality 4 in Fig. 2) in the eastern Arabian Shield yielded a conventional U–Pb zircon age of 645+15/−16 Ma, but also contained a zircon fraction that yielded a U–Pb age of 2067+74/−72 Ma, which Calvez et al. [29] interpreted as evidence for the presence of much older crust in that part of the shield. Kennedy et al. [30], using the ion microprobe, found minor inherited zircon in late Neoproterozoic volcanic rocks in four localities (labelled 5–8 in Fig. 2) across the northern Arabian Shield: andesite/dacite from the central Afif terrane (locality 5), north of the Khida terrane, produced euhedral zircon that yielded mean U–Pb ages of ~630 Ma and inherited cores that yielded U–Pb ages as old as 1869 Ma; rhyolite from the southeastern Hijaz terrane (locality 6) produced euhedral zircon that yielded U–Pb ages of ~740 Ma, some of which contained rounded cores that yielded U–Pb ages of ~2350 and ~1565 Ma; rhyolite from the northeastern Afif terrane (locality 7) produced euhedral zircon yielding tenuous U–Pb ages in the range 490–630 Ma and rounded, possibly detrital zircon that

yielded U–Pb ages up to 2750 Ma, but all of the grains may have experienced isotopic disturbance; and rhyolite from the northwestern Hijaz terrane (locality 8) produced a euhedral zircon population that yielded concordant U–Pb and Pb/Pb ages of ~700 Ma and also produced rounded, probably xenocrystic zircon that yielded ages as old as 1850 Ma. Kennedy et al. [30] interpreted the pre-Neoproterozoic ages as evidence of inheritance from older crustal material. Of particular interest were zircon grains yielding Mesoproterozoic and Archean ages from parts of the shield that are generally accepted as underlain by strictly juvenile Neoproterozoic crust (e.g., Hijaz terrane; Figs. 1 and 2) [30], because crust of Mesoproterozoic age is not exposed within the ANS and the nearest Archean crust is exposed >1200 km to the southeast in Yemen.

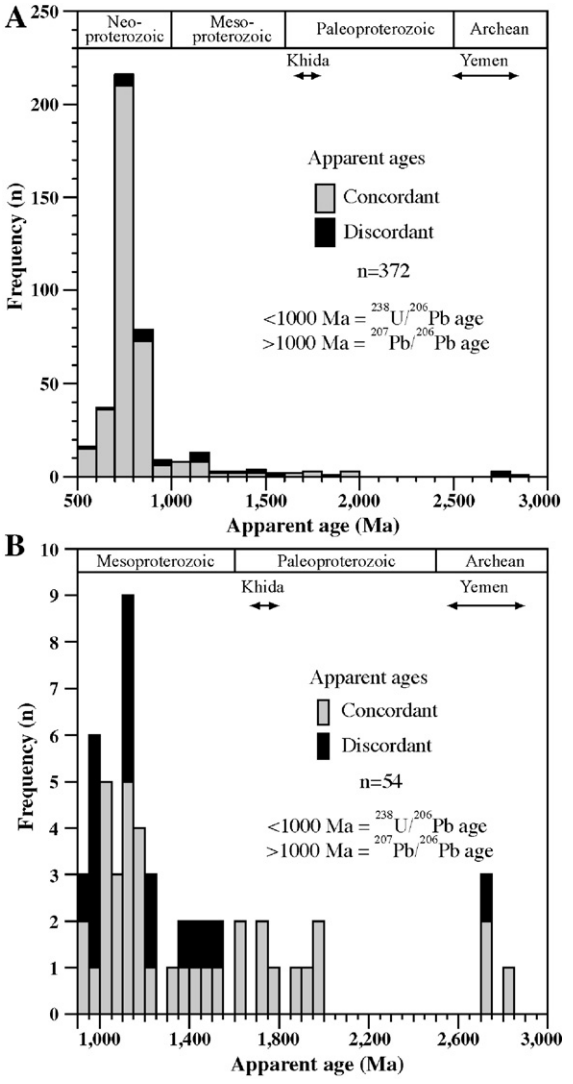


Fig. 3. Histograms of SHRIMP-RG ages of single zircon grains reported by Hargrove et al. [26] and Hargrove [27]: (A) all ages older than 500 Ma; (B) subset of 900–3000 Ma ages. Ages<1000 Ma are $^{238}U/^{206}Pb$ ages and those >1000 Ma are $^{207}Pb/^{206}Pb$ ages. Data sources for zircon ages from the Khida terrane and Yemen basement are provided in the text.

Hargrove et al. [26] and Hargrove [27] also dated non-ophiolitic rocks along the Bi'r Umq suture zone (Figs. 1 and 2) by ion microprobe, and their study revealed the highest concentration of inherited zircon and the oldest inherited zircon ($^{207}Pb/^{206}Pb$ age=2840 Ma) yet reported from the juvenile core of the Arabian Shield. The results of that study are shown in Fig. 3 and are discussed in more detail in Section 3.3. Analytical data and sample descriptions from those studies are available as online addenda (Appendix B) or upon request from the first author.

The present investigation was prompted by the recognition of inheritance and the deficiency in Nd isotopic data over much of the Arabian Shield. Specifically, it seeks to determine if assimilation of older crust is reflected in Nd isotopic signatures of rocks that show significant pre-Neoproterozoic inheritance versus those that do not. Here we report results from Nd isotopic analyses of 31 whole-rock samples from the Bi'r Umq suture zone (Figs. 1 and 2). Combined with information on inheritance throughout the ANS and results from other Nd isotopic studies in the Arabian Shield, the new data are used to establish that the influence of pre-Neoproterozoic crust is probably more widespread in the ANS than is presently appreciated. Although previous workers recognized inheritance in the ANS, they offered little discussion of the implications or possible sources of the contamination.

## 2. Geology of the study areas

The Bi'r Umq suture zone (BUSZ; Figs. 1, 2, 4) is the eastern segment of the larger Bi'r Umq–Nakasib suture zone, a northeast-trending Neoproterozoic fold-and-thrust belt spanning >600 km from eastern Sudan to western Saudi Arabia (configured prior to Cenozoic rifting along the Red Sea). It is the oldest suture zone in the ANS and marks the site of a paleosubduction zone and the collision of the two oldest Neoproterozoic terranes in the ANS: the Gebeit–Hijaz terrane in the north and the Haya–Jeddah terrane in the south (Figs. 1, 2, 4). Thus, the suture zone contains the earliest record of how and when apparently juvenile continental crust in the ANS was formed, assembled, and cratonized. Within the BUSZ in Arabia (Fig. 4), the margins of the Hijaz and Jeddah terranes consist of folded and tectonized ophiolitic nappes, supracrustal assemblages of volcanic, volcaniclastic, and

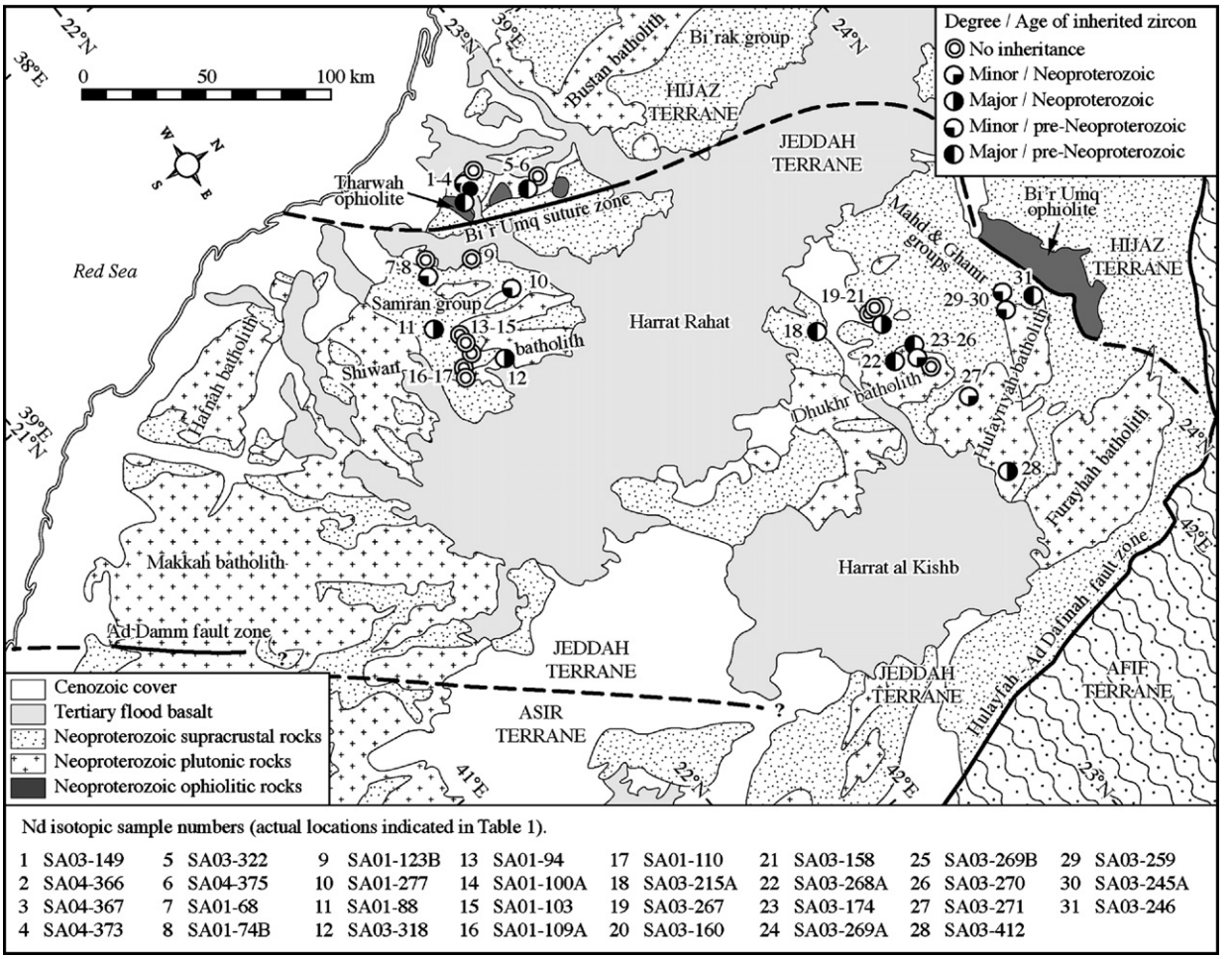


Fig. 4. Geologic map of the study area showing the locations of Nd isotopic samples and the degree and age of inherited zircon. Bold lines denote suture zones and are dashed where inferred.

epiclastic rocks, and voluminous plutonic rocks. Both plutonic and supracrustal rocks were emplaced pre-, syn-, and post-tectonically with respect to suture-related deformation, but different phases of these are not differentiated in Fig. 4.

South of the BUSZ (Fig. 4), the oldest rocks with unequivocal ages are ~800–816 Ma tonalite and trondhjemite in the Dhukhr and Furayhah batholiths in the east and ~800 Ma tonalite of the Shiwan batholith in the west [26,31,32]. Indirect evidence for slightly older plutonic basement in the west comes from the 825 Ma age for zircon from immature arkose most likely derived from the Shiwan batholith [26]. The plutonic basement is unconformably overlain by supracrstal rocks of the 777–760 Ma Mahd and 748 Ma Ghamr groups in the east and by the 777–748 Ma Samran group at the same stratigraphic level in the west [26,31] (Fig. 4). The supracrstal rocks are intruded by 785–760 Ma diorite in the Hufayriyah batholith and 772–769 Ma diorite in the Shiwan batholith (Fig. 4) [26,31,33]. Minor syntectonic tonalites of the Qudayd meta-intrusive suite also intrude the Samran group and their ages constrain the timing of polyphase deformation along the BUSZ between 780 and 750 Ma [26].

North of the BUSZ (Fig. 4), supracrustal rocks in the west belong to the >812 Ma Bi'rak group [26], but stratigraphic equivalents of these are not exposed farther east. The Bi'rak group is intruded by ~807 Ma tonalite in the Bustan batholith [C. Hedge, cited as pers. comm. in [34]]. The Tharwah ophiolite, dated at ~870 Ma by Pallister et al. [25] and at ~777 Ma by Hargrove et al. [26] and Hargrove [27], is surrounded by the Bi'rak group and lies entirely within the Hijaz terrane (Fig. 4). As mentioned previously, the conventional zircon concordia ages of the Tharwah ophiolite are complicated by inheritance and have yet to be resolved. The Bi'r

Table 1
Sm and Nd geochemical and isotopic data for samples from the Bi'r Umq suture zone

| Sample | Code in Fig. 3 | Latitude (°N) | Longitude (°E) | Terrane | Superunit | Lithology | Lithotype | Relation to suturing | Sm (ppm) | Nd (ppm) | $^{147}Sm/^{144}Nd$ | $^{143}Nd/^{144}Nd$ | Initial εNd | Age (Ma) | Model age (Ga)[I] |
|---|---|---|---|---|---|---|---|---|---|---|---|---|---|---|---|
| SA01-068[a] | 7 | 22.4710 | 39.4892 | Jeddah | Qudayd meta-intrusive suite | Metatonalite | P | Syntectonic | 3.98 | 16.11 | 0.149 | 0.512745 | 7.1 | 782 | 0.70 |
| SA01-074B[b] | 8 | 22.4158 | 39.5598 | Jeddah | Samran group-Shayban fm. | Rhyolite | V | Pre-, syntectonic | 1.65 | 5.34 | 0.187 | 0.512827 | 4.9 | 777 | – |
| SA01-088[a] | 11 | 22.3014 | 39.6672 | Jeddah | Misr dike | Syenite | P | Post-tectonic | 1.59 | 10.32 | 0.093 | 0.512485 | 6.6 | 700 | 0.70 |
| SA01-094[b] | 13 | 22.3766 | 39.7374 | Jeddah | Samran group-Amudan fm. | Dacite | V | Pre-, syntectonic | 2.65 | 13.39 | 0.120 | 0.512560 | 6.1 | 753 | 0.77 |
| SA01-100A[b] | 14 | 22.3471 | 39.7582 | Jeddah | Samran group-Amudan fm. | Andesite | V | Pre-, syntectonic | 1.98 | 9.05 | 0.132 | 0.512620 | 6.0 | 750 | 0.78 |
| SA01-103[b] | 15 | 22.3183 | 39.7615 | Jeddah | Samran group-Amudan fm. | Andesite | V | Pre-, syntectonic | 4.04 | 20.80 | 0.117 | 0.512568 | 6.5 | 752 | 0.74 |
| SA01-109A[a] | 17 | 22.2775 | 39.7939 | Jeddah | Nukhu granite | Granite | P | Post-tectonic | 3.42 | 17.92 | 0.115 | 0.512610 | 7.0 | 699 | 0.67 |
| SA01-110[a] | 18 | 22.2548 | 39.8166 | Jeddah | Kamil intrusive suite | Diorite | P | Pre-, syntectonic | 2.73 | 9.89 | 0.167 | 0.512818 | 6.8 | 802 | 0.72 |
| SA01-123B[a] | 9 | 22.5517 | 39.5902 | Jeddah | Qudayd meta-intrusive suite | Metatonalite | P | Syntectonic | 3.10 | 10.53 | 0.178 | 0.512869 | 6.6 | 751 | 0.72 |
| SA03-149[a] | 1 | 22.6405 | 39.3950 | Hijaz | Tharwah ophiolite | Gabbro | O | Pretectonic | 0.71 | 1.32 | 0.325 | 0.513643 | 5.6 | 870[c] | - |
| SA03-149[a] | 1 | 22.6405 | 39.3950 | Hijaz | Tharwah ophiolite | Gabbro | O | Pretectonic | 0.71 | 1.32 | 0.325 | 0.513643 | 7.1 | 777 | - |
| SA03-158[a] | 22 | 23.4232 | 40.6581 | Jeddah | Mahd group- Haf fm. | Rhyolite | V | Pre-, syntectonic | 7.89 | 33.18 | 0.144 | 0.512711 | 6.9 | 777 | 0.71 |
| SA03-160[a] | 21 | 23.4335 | 40.6600 | Jeddah | Ramram intrusive complex | Granodiorite | H | Pre-, syntectonic | 6.41 | 29.32 | 0.132 | 0.512714 | 8.1 | 769 | 0.61 |
| SA03-174[b] | 24 | 23.5014 | 40.8377 | Jeddah | Mahd group- Haf fm. | Rhyolite | V | Pre-, syntectonic | 2.88 | 11.36 | 0.154 | 0.512730 | 6.3 | 776[f] | 0.78 |
| SA03-215A[b] | 19 | 23.2423 | 40.5561 | Jeddah | Mahd group- Haf fm. | Basaltic andesite | V | Pre-, syntectonic | 2.87 | 10.39 | 0.167 | 0.512787 | 6.1 | 776[f] | 0.81 |
| SA03-245A[a] | 31 | 23.7962 | 40.9393 | Jeddah | Raghiyah intrusive suite | Granodiorite | P | Post-tectonic | 24.65 | 103.60 | 0.144 | 0.512677 | 4.9 | 573[d] | 0.79 |

| | | | | | | | | | | | | | | | |
|---|---|---|---|---|---|---|---|---|---|---|---|---|---|---|---|
| SA03-246[b] | 32 | 23.8689 | 40.9684 | Jeddah | Raghiyah intrusive suite | Granodiorite | P | Post-tectonic | 8.07 | 38.79 | 0.126 | 0.512559 | 3.9 | 573[d] | 0.83 |
| SA03-259[b] | 30 | 23.8218 | 40.9105 | Jeddah | Arj group | Basaltic andesite | V | Pretectonic | 1.19 | 3.35 | 0.215 | 0.513018 | 5.8 | 785[g] | – |
| SA03-267[a] | 20 | 23.4578 | 40.6661 | Jeddah | Ramram intrusive complex | Granite | H | Pre-, syntectonic | 6.53 | 30.28 | 0.130 | 0.512734 | 8.5 | 749 | 0.56 |
| SA03-268A[a] | 23 | 23.4156 | 40.8152 | Jeddah | Mahd group intrusion | Dacite | H | Pre-, syntectonic | 2.75 | 13.50 | 0.123 | 0.512561 | 6.0 | 776[d] | 0.80 |
| SA03-269A[a] | 25 | 23.4154 | 40.8162 | Jeddah | Dhukhr tonalite | Metatonalite | P | Pretectonic | 0.49 | 2.58 | 0.116 | 0.512527 | 6.4 | 803 | 0.79 |
| SA03-269B[a] | 26 | 23.4154 | 40.8162 | Jeddah | Mahd group intrusion | Rhyolite | H | Pre-, syntectonic | 10.00 | 35.80 | 0.169 | 0.512799 | 6.1 | 771 | 0.81 |
| SA03-270[a] | 27 | 23.4770 | 40.9256 | Jeddah | Bari granodiorite | Granite | P | Pre-, syntectonic | 2.54 | 12.00 | 0.128 | 0.512642 | 7.2 | 776 | 0.71 |
| SA03-271[a] | 28 | 23.5031 | 41.0586 | Jeddah | Hufayriyah tonalite | Tonalite | P | Pre-, syntectonic | 3.06 | 13.85 | 0.134 | 0.512671 | 7.2 | 785 | 0.70 |
| SA03-277[b] | 10 | 22.5778 | 39.7486 | Jeddah | Samran group-Shayban fm. | Dacite | V | Pre-, syntectonic | 2.04 | 6.22 | 0.198 | 0.512944 | 6.1 | 777[h] | – |
| SA04-318[a] | 12 | 22.4122 | 39.8883 | Jeddah | Kamil intrusive suite | Diorite | P | Pre-, syntectonic | 2.27 | 11.12 | 0.124 | 0.512594 | 6.6 | 772 | 0.75 |
| SA04-322[a] | 5 | 22.9033 | 39.4745 | Hijaz | Rabigh suite | Granodiorite | P | Pretectonic | 2.83 | 12.47 | 0.137 | 0.512680 | 7.2 | 807[e] | 0.71 |
| SA04-366[b] | 2 | 22.7056 | 39.3660 | Hijaz | Bi'rak group | Microgabbro | V | Pretectonic | 3.10 | 9.90 | 0.189 | 0.512933 | 6.8 | 854 | – |
| SA04-367[b] | 3 | 22.7050 | 39.3620 | Hijaz | Bi'rak group | Microgabbro | V | Pretectonic | 4.60 | 16.60 | 0.168 | 0.512830 | 7.0 | 812 | 0.69 |
| SA04-373[a] | 4 | 22.7768 | 39.3243 | Hijaz | Hanak granite | Granite | P | Post-tectonic | 6.23 | 40.09 | 0.094 | 0.512503 | 5.4 | 596 | 0.68 |
| SA04-375[a] | 6 | 22.8331 | 39.4790 | Hijaz | Rabigh suite | Diorite | P | Pretectonic | 2.72 | 10.91 | 0.151 | 0.512704 | 6.3 | 807[e] | 0.81 |
| SA04-412[a] | 29 | 23.4450 | 41.3943 | Jeddah | Dhukhr tonalite | Quartz diorite | P | Pretectonic | 3.21 | 12.97 | 0.150 | 0.512708 | 6.5 | 813 | 0.78 |

All isotopic analyses conducted at UT Dallas on a Finnigan MAT 261 solid-source instrument. Trace element concentrations determined at [a] Shimane University, Japan and [b] The University of Texas at Dallas. Age data from Hargrove et al. [26] and Hargrove [27], except for: [c] U–Pb zircon age from Pallister et al. [25]; [d] Rb–Sr whole-rock isochron age from Calvez and Kemp [31]; [e] U–Pb zircon age from C. Hedge (cited as pers. comm. in [34]). [f] Maximum age of Mahd gp.; [g] Minimum age based on age of intruding Hufayriyah tonalite; [h] Maximum age for Shayban fm. [g] Model ages based on DePaolo [37]. P=Plutonic; H=Hypabyssal; V=Volcanic; O=Ophiolitic.

Umq ophiolite in the east (Fig. 4), dated at ~840–830 Ma [25], was thrust directly onto the Jeddah terrane over the Mahd group.

Late syntectonic to post-tectonic, supracrstal rocks unconformably overlie deformed units to the north and south of the suture, but are not differentiated in Fig. 4. Related post-tectonic intrusions, mostly alkaline to peralkaline granitoids, punctuated the region between ~700 and 520 Ma (e.g., [17,26,31,35]) and are included as minor parts of the batholiths in Fig. 4. They represent the last major magmatic episode to affect the Arabian Shield until Cenozoic rifting along the Red Sea.

Thirty-one samples ranging in age from 573 to 870 Ma were selected from pre-and syntectonic intrusive and contemporaneous volcanic rocks and from a suite of post-tectonic granitoids. U–Pb zircon crystallization ages were obtained for most samples by ion microprobe at Stanford University. Data from the analyses are available as online addenda (Appendix B) or upon request from the first author and are discussed in more detail in Hargrove et al. [26] and Hargrove [27]. Several samples not dated directly by those authors are parts of units from which other samples yielded acceptable ages. The Tharwah ophiolite is indicated in some figures with both the 870 Ma age determined by Pallister et al. [25] and the 777 Ma age obtained by Hargrove et al. [26] and Hargrove [27]. Calvez and Kemp [31] obtained a Rb–Sr whole-rock isochron age for the post-tectonic granitoid suite. Analytical techniques for sample decomposition and isotopic analyses are given in Appendix A.

## 3. Results and discussion

Trace element concentrations and Sm and Nd isotopic data are presented in Table 1. The samples show wide ranges in Sm (0.49–24.65 ppm) and Nd (1.32–103.6 ppm) concentrations. The wide range in $^{147}Sm/^{144}Nd$ (0.0928–0.3248) is more likely due to variable enrichment in the light rare earth elements associated with evolution of the parental magmas than to significant differences in the compositions of the magma sources. Exceptions include the post-tectonic granitoids and the Ramram intrusive complex, and the reasons for their exceptions are discussed below. Initial $^{143}Nd/^{144}Nd$ for samples analyzed during this study range from 0.511790 to 0.512137.

### 3.1. Epsilon Nd

Initial epsilon Nd ($\varepsilon_{Nd}(T)$) for the 31 BUSZ samples were calculated by adjusting the isotopic values for the chondritic uniform reservoir to the La Jolla Nd standard ($^{143}Nd/^{144}Nd = 0.511847$, [36]) and are plotted against time in Fig. 5, along with data recalculated from the literature for samples from the Arabian Shield. Most of the BUSZ samples show highly positive $\varepsilon_{Nd}(T)$ (+3.9 to +8.5) and plot within the shaded field defined by ANS "oceanic" terranes (Fig. 5), which is in sharp contrast to strongly negative $\varepsilon_{Nd}(T)$ of the Khida terrane in the eastern shield (Figs. 2 and 5). The fact that most BUSZ samples plot within 1 epsilon unit of the model depleted-mantle curve of DePaolo [37] in Fig. 5 suggests that the crust along the BUSZ is juvenile and was derived from melting of depleted mantle with an isotopic composition similar to that predicted by DePaolo [37]. However, there are several notable exceptions. (1) Despite field and geochronological evidence indicating that subvolcanic rocks of the Ramram complex are consanguineous with pyroclastic-flow deposits of the Mahd group (Fig. 4) [26], Ramram samples (SA03-160, SA03-267) show atypically high $\varepsilon_{Nd}(T)$ and straddle the depleted mantle curve of Goldstein et al. [38] (Fig. 5B), whereas samples of the Mahd group and most other contemporary units plot within the main grouping of points along the DePaolo curve. This may reflect progressive depletion of a common source in the time between extrusion of the Mahd group and emplacement of the Ramram intrusions. (2) The notably lower $\varepsilon_{Nd}(T)$ of a sample from the Samran group (SA01-74B) compared to contemporary samples (Fig. 5B) suggests that parts of the Samran group were derived from a more enriched source, as reflected in that sample's anomalously high model age and as discussed in the following Section. (3) The $\varepsilon_{Nd}(T)$ data for three post-tectonic granitoids (SA03-245A, SA03-246, SA04-373) show a significant departure from the DePaolo curve (Fig. 5B), but fall along a line that approximates the $\varepsilon_{Nd}(T)$ growth curve of BUSZ crust. This supports conclusions of previous studies (e.g., [39,40]) that similar post-tectonic A-type granitoids with elevated $^{87}Sr/^{86}Sr$ and peralkaline chemistries originated by anatexis of the lower crust, possibly as a result of thickening during continental collision along the East African Orogen. Alternatively, the granitoids were derived from mafic magmas generated by partial melting of more enriched asthenosphere than were BUSZ samples that underwent extensive subsequent fractional crystallization. In contrast to the post-tectonic granitoids, two post-tectonic syenitic–gabbroic megadikes (SA01-88, SA01-109A) yield $\varepsilon_{Nd}(T)$ comparable to the majority of BUSZ samples (Fig. 5B), which suggests that the dikes were derived from a source with similar elemental and isotopic compositions as that from which most older samples were derived.

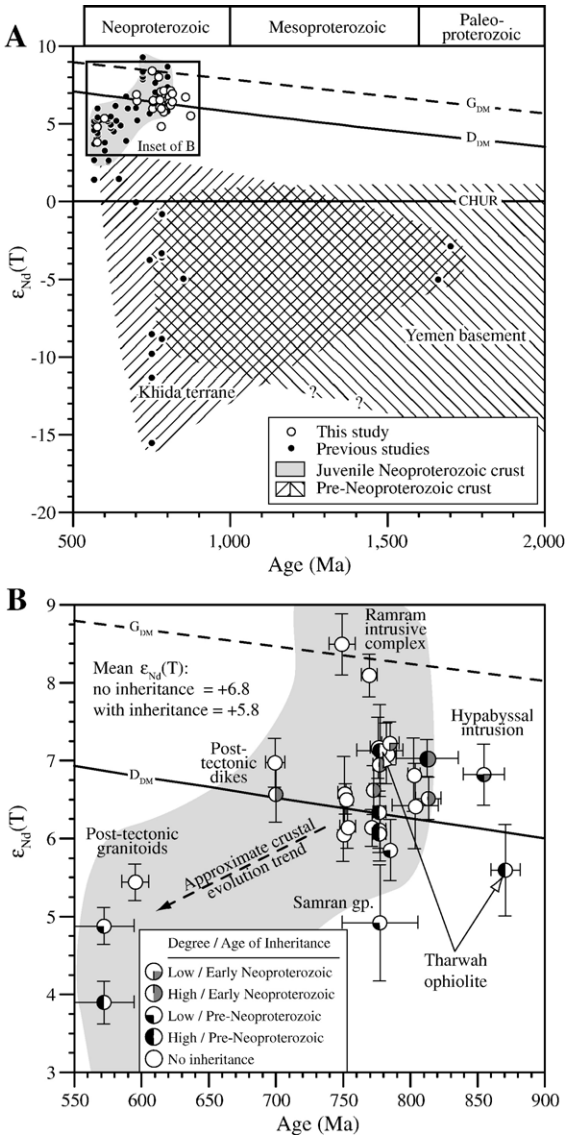


Fig. 5. Plots of initial epsilon Nd versus crystallization age: (A) for all data for Proterozoic rocks of the Arabian Shield from this and previous studies and (B) for Neoproterozoic rocks along the Bi'r Umq suture zone (this study), showing degrees of zircon inheritance and two-sigma error bars for epsilon Nd and age. Also shown are the reference line for the chondritic uniform reservoir (CHUR) and the depleted mantle evolution curves of: $D_{DM}$, DePaolo [37]; and $G_{DM}$, Goldstein et al. [38]. The field for basement gneisses in Yemen is well constrained by Nd isotopic data but poorly constrained by radiometric ages. Additional data sources: Agar et al. [65], Duyverman et al. [72], Hegner and Pallister [69], Stacey and Hedge [18], and Stoeser and Frost [58]. Ages for samples analyzed during this study are from Hargrove et al. [26] and Hargrove [27]. Alternative data points for the Tharwah ophiolite are based on the 870 Ma age by Pallister et al. [25] and the 777 Ma age by Hargrove et al. [26] and Hargrove [27]. Explanatory text indicating lithology refers to data from this study only. Samples showing no inheritance are placed behind those with inheritance. Time scale divisions are from Gradstein et al. [3].

The two points for Tharwah ophiolite gabbro are based on the conflicting 870 Ma [25] and 777 Ma [26] ages. As the younger age is preferred as a crystallization age, the correspondingly higher $\varepsilon_{Nd}(T)$ (+7.1) is also preferred and is indistinguishable from that of most other BUSZ samples generally interpreted as arc rocks.

### 3.2. Model ages

For this study we assumed that juvenile magmatic additions to BUSZ crust originated primarily by partial melting of depleted asthenosphere and that the timing of melting can be estimated by calculating a Nd model age ($T_{DM}$), which indicates when the initial $^{143}Nd/^{144}Nd$ of a sample was equal to that of its depleted mantle source. Model ages (Table 1) were calculated using the model for depleted mantle isotopic compositions of DePaolo [37], which is preferred over the models of Goldstein et al. [38] and others because it more accurately reflects the $\varepsilon_{Nd}(T)$ of non-ophiolitic rocks that were interpreted as juvenile from independent evidence and because it provides a more realistic prediction of the $\varepsilon_{Nd}(T)$ for the source of arc-related rocks. Curves showing the evolution of depleted mantle modelled by DePaolo [37] and Goldstein et al. [38] are shown in Fig. 5.

Samples with high Sm/Nd produce unreliable model ages, because the slope of the $^{147}Sm/^{144}Nd$ evolution curve approaches that of depleted mantle, resulting in large errors on the intercept of the two curves or, in some

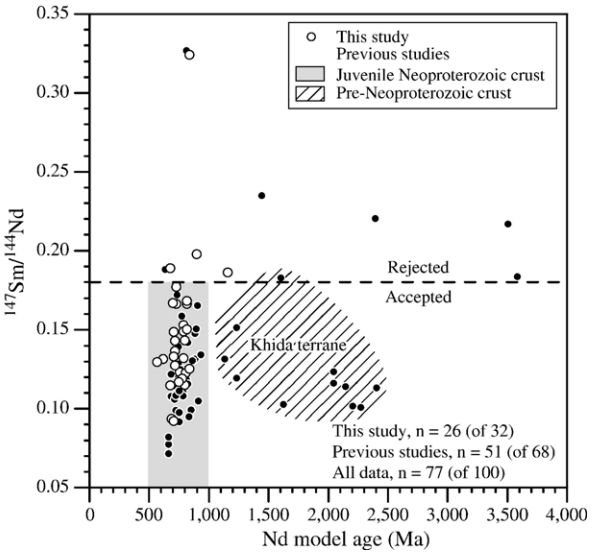


Fig. 6. Plot of $^{147}Sm/^{144}Nd$ vs. Nd model age (model of DePaolo [37]). Samples with $^{147}Sm/^{144}Nd > 0.180$ do not yield reliable model ages and are excluded from model age calculations. Data in plot were filtered for unrealistic or geologically impossible model ages (i.e. model age ≪ crystallization age or model age > age of Earth).

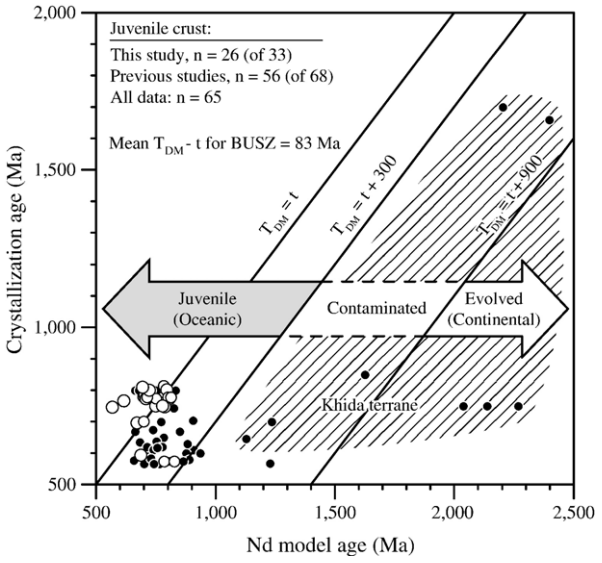


Fig. 7. Plot of Nd model age ($T_{DM}$) vs. crystallization age ($t$), modified from Harris et al. [42]. Data that yield $T_{DM}=t$ or $T_{DM}<t+300$ are considered to come from juvenile (oceanic) crust, those producing $T_{DM}>t+900$ are considered to come from evolved (continental) crust, and those with $t+300<T_{DM}<t+900$ are from juvenile crust contaminated by evolved crust. Data for crystallization ages are from Hargrove et al. [26] and Hargrove [27], and the depleted mantle model is that of DePaolo [37].

cases, no intercept or geologically impossible intercepts. Which samples should be excluded depends upon the data set (cf. [7,41]). We used the graphical filter shown in Fig. 6, which plots $T_{DM}$ against present $^{147}Sm/^{144}Nd$. Most samples from the Arabian Shield show little variation in $T_{DM}$ with increasing $^{147}Sm/^{144}Nd$, as indicated by the shaded region, except for samples from within or along the periphery of the Khida terrane (Fig. 2). However, samples with $^{147}Sm/^{144}Nd>0.180$ show marked variation in $T_{DM}$ at similar $^{147}Sm/^{144}Nd$ and were excluded from the calculations and further discussion, as were samples yielding geologically unrealistic $T_{DM}$ (i.e. that post-date the youngest igneous events in the Arabian Shield (~500 Ma) or that predate the age of the Earth). In total, 26 of 32 samples from the BUSZ and 51 of 68 samples from previous studies passed these filters. Surviving data from the BUSZ yield reliable $T_{DM}$ ages in the range 560–830 Ma (Table 1). One sample that did not pass the filters was from the Samran group (SA01-74B). Recall that this sample yielded lower $\varepsilon_{Nd}(T)$ than most contemporary samples (Fig. 5B) and an anomalously high $T_{DM}$ (1150 Ma). Although unreliable, both the $T_{DM}$ and $\varepsilon_{Nd}(T)$ suggest that the Nd isotopic system of that sample was contaminated by older, more radiogenic material.

Model ages approximate the U–Pb zircon crystallization ages of most BUSZ samples (Table 1), which supports the assertion that much of the Arabian Shield crust is juvenile. We quantitatively define juvenile crust by comparing crystallization and model ages (Fig. 7) to distinguish juvenile (oceanic) from evolved (continental) crust in the Arabian Shield. Samples for which model ages are within 300 Ma of crystallization ages are assumed to be juvenile, because little time elapsed between extraction of the parental melts from the mantle and crystallization of felsic melts (anatectic and/or differentiated) [42]. Such is the case for most samples from the Arabian Shield and all BUSZ samples, the latter of which show a mean difference between model and crystallization ages of 83 Ma. As shown in Fig. 8, the range of model ages for BUSZ samples is 560–830 Ma (mean=740 Ma) and for the entire Arabian Shield, including the Khida terrane, is 560–2400 Ma (mean=900 Ma). Excluding the Khida terrane, the mean model age for the shield falls to 770 Ma, which is comparable to the means from other parts of the ANS

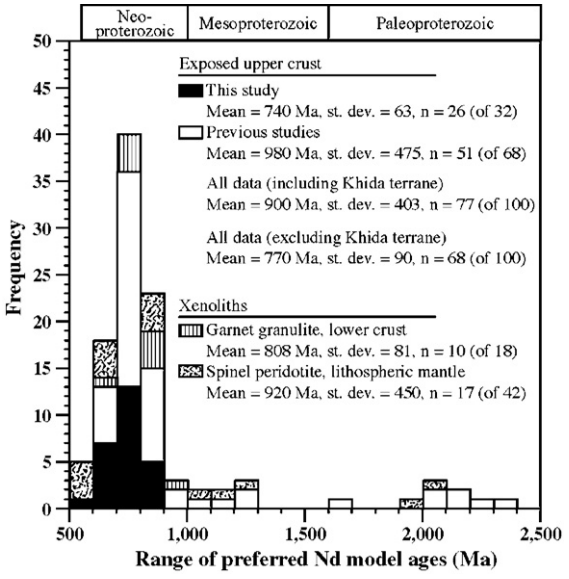


Fig. 8. Histogram of Nd model ages (model of DePaolo [37]) for upper crustal rocks and xenoliths from the lower crust and lithospheric mantle of the Arabian Shield, showing the data from this study and data recalculated from the literature, including Agar et al. [65], Duyverman et al. [72], Hegner and Pallister [69], Stacey and Hedge [18], Henjes-Kunst et al. [10], McGuire and Stern [11], and Stoeser and Frost [58]. Data for the granulite xenoliths show an increase in model age with increasing $^{147}Sm/^{144}Nd$, and samples with $^{147}Sm/^{144}Nd>0.170$ were excluded from model age calculations. Data for the peridotite xenoliths do not show a correlation between model age and $^{147}Sm/^{144}Nd$ and were not filtered for such. The mean values for the sample populations±1 standard deviation are given. Time scale divisions are from Gradstein et al. [3].

considered to be juvenile, including eastern Sudan (760 Ma), eastern Egypt (740 Ma), Israel–Jordan–Sinai (840 Ma), and Eritrea and northern Ethiopia (870 Ma) ([7], and references therein).

The juvenile nature of upper crust exposed in Arabia is established from existing isotopic data, and a similar case can be made for the lower crust and lithospheric mantle beneath the shield. Samples of garnet granulite and spinel peridotite, which were exhumed by Tertiary basalts in Saudi Arabia, show a comparable spread of model ages to exposed crust (Fig. 8). Data for granulite xenoliths [11] show a noticeable increase in $T_{DM}$ with increasing $^{147}Sm/^{144}Nd$, and samples with $^{147}Sm/^{144}Nd > 0.170$ were excluded from calculations. The remaining data yield model ages of 700–1240 Ma, with a mean (808 Ma) that is slightly higher than that for juvenile parts of the shield (Fig. 8). The combined data suggest that the entire 40-km-thick crust beneath much of the Arabian Shield was extracted from the mantle in the interval 550–870 Ma, and most of it was extracted between 740 and 830 Ma. Data for peridotite xenoliths [10,12] show no correlation between $T_{DM}$ and $^{147}Sm/^{144}Nd$ and were not filtered for such. However, only 17 yield geologically possible model ages, and because of significant scatter in the data not correlated with $^{147}Sm/^{144}Nd$ we recognize that some of the older model ages for the peridotites may be unreliable. The peridotites show a much wider range in $T_{DM}$ (600–1950 Ma) than the granulites, but a mean (846 Ma) that is comparable.

### 3.3. Inheritance

Overall, the Nd isotopic data support previous assertions that the core of the ANS is juvenile Neoproterozoic crust, but this conclusion is premature in light of the Mesoproterozoic–Archean zircon grains inherited by isotopically juvenile Neoproterozoic rocks along the BUSZ and elsewhere in the ANS. The ages of those grains are comparable to model ages for upper crust rocks and xenoliths from the lower crust and mantle lithosphere. Of the ~400 zircon grains analyzed by Hargrove et al. [26] and Hargrove [27], 86% yielded Neoproterozoic ages in the range (900–540 Ma) expected from previous dating campaigns and currently accepted models for ANS formation (Fig. 3A) and 14% yielded ages older than expected for juvenile ANS crust (Fig. 3A, B). The older-than-expected (i.e. inherited) ages include 12 early Neoproterozoic, 31 Mesoproterozoic, 9 Paleoproterozoic, and 4 Archean ages (Fig. 3B). Pre-Neoproterozoic inherited zircon grains occur in the Tharwah ophiolite, pre-and syntectonic volcanic rocks, and post-tectonic granitoids, but most occur in volcanic rocks with crystallization ages of 785–750 Ma [26]. Samples with inherited zircon show slightly lower Nd concentrations, lower initial $^{143}Nd/^{144}Nd$, and therefore

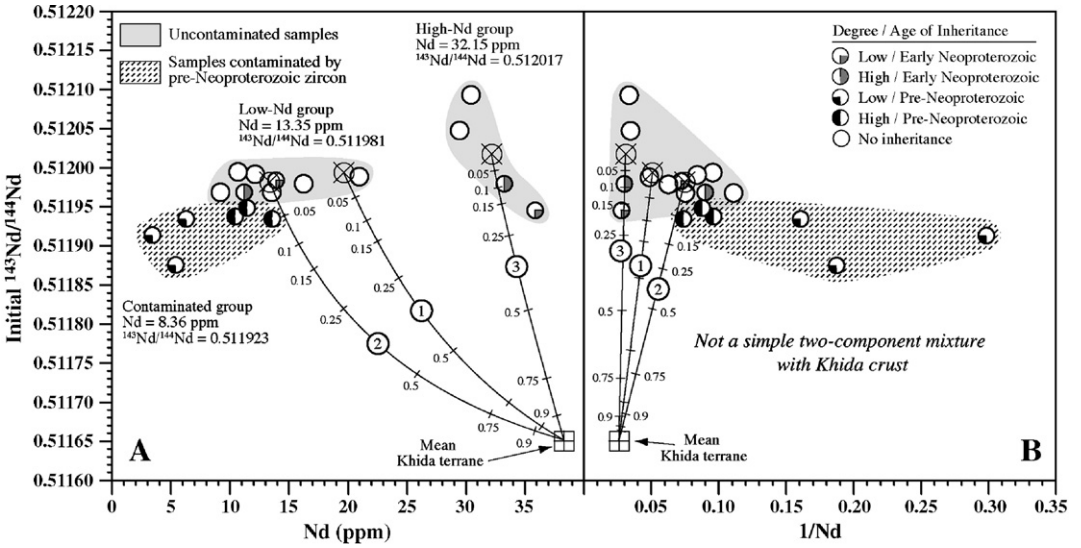


Fig. 9. Plots of initial $^{143}Nd/^{144}Nd$ vs. Nd concentration for BUSZ samples in the age range ~785–750 Ma, in which most pre-Neoproterozoic inheritance occurs. Two-component (A) hyperbolic and (B) linear trajectories are shown for ideal mixtures between the mean composition for samples from the Khida terrane and the means for samples with no pre-Neoproterozoic inherited zircon from the BUSZ. Trajectories for (1) all samples, (2) low-Nd samples only, and (3) high-Nd samples only, reflect increasing contamination by Khida-type crust, with numbers representing fraction of assimilation. The mean Nd elemental and isotopic compositions of high-Nd and low-Nd uncontaminated samples and for the contaminated samples are given. Important note: the diagram illustrates that inheritance is not due to mixing with crust that is chemically like the Khida terrane.

lower $\varepsilon_{Nd}(T)$ than contemporaneous samples that lack inherited zircon (Figs. 5 and 9). One explanation for this is contamination of juvenile magmas by material that contained older zircon and had more evolved Nd isotopic compositions, the nearest possible source of which is the Khida terrane (Fig. 2). If samples with pre-Neoproterozoic zircon were contaminated by material with the average composition of Khida crust, then they should plot along the mixing lines in Fig. 9. The fact that they do not indicates that they are not simple two-component mixtures and/or that the Khida terrane is not the source of the contamination. The latter is supported by the abundance of Mesoproterozoic inherited zircon in BUSZ rocks and the apparent absence of Mesoproterozoic crust in the Khida terrane, or anywhere else in the ANS. However, the possibility that crust of appropriate age exists elsewhere in the Arabian craton (i.e. concealed beneath Phanerozoic cover) is acknowledged.

No correlation exists between the amount of inherited zircon in a sample and the magnitude of $\varepsilon_{Nd}(T)$, as might be expected if more radiogenic crust was assimilated, but this may partly reflect sampling bias. Hargrove et al. [26] and Hargrove [27] focused on acquiring crystallization ages for igneous units and targeted juvenile zircon crystals. Had both juvenile and xenocrystic zircon been targeted equally, the number of pre-Neoproterozoic grains analyzed probably would have been greater. Alternatively, the lack of correlation could be a function of the dependence of inherited zircon preservation on zirconium saturation temperatures in the host magmas (e.g., [43]), but this has not been quantitatively tested for our samples. Nonetheless, the combination of slightly lower $\varepsilon_{Nd}(T)$ and inherited zircon suggests that some juvenile magmas emplaced along the BUSZ assimilated some older material with more radiogenic initial $^{143}Nd/^{144}Nd$ and lower $\varepsilon_{Nd}(T)$. Exactly how much assimilation occurred is difficult to ascertain because of the small differences in mean Nd elemental (5 ppm) and isotopic (0.000058) compositions between samples with significant inheritance and those without (Figs. 5B and 9). We therefore suggest that some magmas assimilated enough older crust to inherit abundant zircon, but not enough to significantly affect $\varepsilon_{Nd}(T)$.

The growing number of studies that document inheritance suggests that the influence of pre-Neoproterozoic continental material was not confined to the Afif terrane and crust with evolved Pb (Fig. 2), but was important in the "juvenile" oceanic core of the shield as well. The extent of that influence is approximated in Fig. 1 by the "contaminated shield," which encloses almost one-third of the ANS. It should be noted, however, that the outline of the contaminated shield encloses two areas of contaminated juvenile crust that are separated by the Hulayfah–Ad Dafinah fault zone. These two areas were likely separated by significant distances at the time of contamination and since have been juxtaposed.

### 3.3.1. Sources of the inheritance

As important as understanding the extent of pre-Neoproterozoic continental material in the ANS is determining the source of the contaminant material. Hargrove et al. [26] and Hargrove [27] discounted the likelihood of inadvertent contamination in the laboratory, which is supported by the recognition of inheritance by other workers (e.g., [25,30]). Therefore, the problem is how isotopically juvenile Neoproterozoic magmas were contaminated with pre-Neoproterozoic zircon. Was zircon acquired from unexposed older crust that underlies the contaminated shield (Fig. 9) or derived from Neoproterzoic sediments sourced from a neighboring pre-Neoproterozoic craton?

The fact that most inherited zircon from the "juvenile" Arabian Shield yields early Neoproterozoic and Mesoproterozoic U–Pb ages [25,26,30] and that many samples from the ANS yield comparably old Nd model ages suggests that crust in that age range is the primary source of contamination. However, no crust older than ~890 Ma [44] is exposed in the juvenile core of the ANS, and crust of Mesoproterozoic age is not exposed anywhere in the ANS. In their study of detrital zircon from Cambrian sandstones in Israel, Avigad et al. [45] attributed the source of 550–650 Ma zircon to the ANS and the source of 1650–1850 Ma and 2450–2700 Ma zircon to the more distant Afif terrane to the southeast and Saharan metacraton to the southwest, each ~1000 km distant. The source of 900–1100 Ma zircon is more problematic, because the nearest crust of that age is exposed >3000 km to the south in central and eastern Africa. Avigad et al. [45] suggested that such long-travelled zircon may have been fluvially transported, but morphologies are more characteristic of grains that were either locally derived or transported intact by other processes (e.g., by glaciers).

A sedimentary origin for inherited zircon from the BUSZ is partly supported by morphological characteristics. Most of the inherited grains analyzed by Hargrove et al. [26] and Hargrove [27] are rounded or have rounded cores enclosed by more euhedral overgrowths. Roundness is consistent with a detrital origin, but can also arise from partial magmatic resorption. If some zircon was incorporated as sediment, a fertile source region is required to account for the age range of inherited zircon from the BUSZ. Candidates with

appropriate ages and isotopic compositions include Paleoproterozoic–Archean crust of the Saharan Metacraton, the Khida terrane, and basement in Yemen (Figs. 1 and 2), but a source of Meosproterozoic zircon within these cratonic areas is presently unknown. It should be noted that at the time the zircon was inherited (i.e. the time of igneous crystallization), which was prior to or during accretion of the juvenile terranes, the positions of these potential sources relative to the BUSZ may have been even more distant than at present.

One possible mechanism for inheritance by assimilation of terrigenous clastic sediment (including detrital zircon or zircon contained within lithic clasts) involves the shedding of sediment from nearby passive margins, accumulation of the sediment on the seafloor upon which the Jeddah and Hijaz arc terranes were later constructed, and subsequent entrainment in juvenile arc magmas. Highly deformed sedimentary sequences in the Central Eastern Desert (CED) [46] and the Sinai [47] (Figs. 1 and 2) are interpreted as accretionary prisms. Also, some metavolcanic rocks in the CED, which yield maximum Nd model ages of ~800 Ma and strongly positive $\varepsilon_{Nd}(T)$, are interlayered with clastic metasedimentary rocks that yield Mesoproterozoic Rb–Sr whole-rock isochron ages, Paleoproterozoic Nd model ages, and strongly negative $\varepsilon_{Nd}(T)$ [48]. Both cases argue for concomitant clastic sedimentation and arc volcanism in the core of the ANS.

An alternative mechanism involves glacial erosion and deposition of sediments from various source regions and subsequent scavenging of those sediments by shallow-level magmas. Support for this mechanism is provided by deposits in the region that are attributed to major episodes of Neoproterozoic glaciation [e.g., [49–52]]. In the BUSZ, diamictite separating the 800–816 Ma Dhukhr batholith from the overlying 776 Ma Mahd group (Fig. 4) may record glaciation comparable in age to the Kaigas event (780–740 Ma) (e.g., [53]) in Namibia. Tillites are likely to contain enough zircon with disparate provenance to account for the variety in ages and number of inherited grains observed by Hargrove et al. [26] and Hargrove [27]. This argument is not preferred, however, because the diamictite is <3 m thick, is discontinuously exposed, and correlative units are not exposed in the stratigraphy west of Harrat Rahat shown in Fig. 4, where some of the inheritance occurs.

Although sedimentary origins for the inherited zircon are possible, some inherited grains exhibit characteristics more consistent with juvenile crystals, such as euhedral morphologies and a lack of recognizable cores, which suggest that some grains were assimilated in situ from their original host igneous rocks (i.e. from cryptic pre-Neoproterozoic crust). Moreover, arguments invoking sedimentary sources for inherited zircon do not adequately account for inheritance in the Tharwah ophiolite, which was an impetus for the present study because it presents a distinct problem: Ophiolites form by decompression melting of asthenosphere during seafloor spreading, and the incorporation of pre-existing crustal material into asthenospheric melts is difficult to reconcile unless rifting of continental crust is involved. Such a model was suggested for the Bi'r Umq–Nakasib suture zone by Abdelsalam and Stern [54] and is supported by the findings of Hargrove et al. [26] and Hargrove [27]; Johnson et al. [55,56] interpret the BUSZ suture zone as resulting from the accretion of the Jeddah and Hijaz arc terranes, but do not interpret the origins of the intervening ocean basin. Thus, inheritance in an ophiolite seems to require the presence of older crust where ophiolitic magmas are emplaced, which is an additional mechanism that we suggest for the origin of at least some of the inherited zircon. Just as the Khida terrane (Fig. 2) is the foundation upon which some of the Afif arc terrane was constructed, there may be older, yet cryptic basement to the Hijaz–Gebeit and Jeddah–Haya arc terranes from which juvenile arc magmas extracted pre-Neoproterozoic zircon. Although this cryptic basement may be a source of contaminant zircon, it did not significantly impact the Nd isotopic systematics of the younger arc rocks.

More direct evidence for older basement in the core of the ANS may come from Zabargad Island, off the southeast coast of Egypt. Granulite gneisses there yield metamorphic dates of 669±34 Ma (Sm–Nd) and 655±8 Ma (Rb–Sr), but initial Nd isotopic data were interpreted to indicate extraction of the protoliths from depleted mantle after 1200 Ma, and possibly as early as 1700 Ma [57]. Those model ages are comparable to Mesoproterozoic ages for inherited zircon in the Arabian Shield [26,30]. Post-tectonic granites in the CED and BUSZ that contain inherited zircon are possibly anatectic melts of that or a similar continental component [23]; however, fusion of mafic lower crust as a source for the pre- and syntectonic units, which contain the bulk of the inherited zircon, is discounted because no correlation exists between adakitic chemistries and inheritance [27] in the BUSZ samples.

The age of the cryptic basement, if it exists, is inferred from the ages of inherited zircon grains to be dominantly Mesoproterozoic, with subordinate Paleoproterozoic and rare Archean components (Fig. 3B). The present extent of that basement may be approximated by the "contaminated shield" in Fig. 9, where inheritance of pre-Neoproterozoic zircon is

documented. It should be noted, however, that available Pb and Nd isotopic data, including those presented herein, do not support the existence of widespread cryptic basement beneath the core of the ANS, although widely variable initial Sr isotopic ratios argue for a widespread source of contamination (see [58]). At the very least, the data support local mixing of juvenile Neoproterozoic magmas with more isotopically evolved material, such as localized deposits of terrigenous sediment, highly attenuated crust, or continental microplates of pre-Neoproterozoic age.

### 3.4. Implications for tectonic models

If the ANS proves less juvenile than previously thought, then revision is required of the estimates of crustal accretion rates that cite the ANS as a model for juvenile continental crust generation in the Neoproterozoic or for understanding modern processes of crust formation. For example, Reymer and Schubert [59] modelled growth rates in the ANS up to 310 $km^3\ km^{-1}\ Ma^{-1}$, which is an order of magnitude greater than the rates estimated for arcs since the end of the Paleozoic. To account for such anomalously rapid rates, some authors (e.g., [60,61]) suggested that ANS assembly involved the accretion of oceanic plateaux as well as arc terranes, because plateaux are the largely unsubductable surface expressions of voluminous juvenile lithosphere emplaced by mantle plumes over brief time periods. Other authors [e.g., sai [5]] model normal growths rates that rely on the involvement of pre-existing continental crust. The role of older crust is arguably supported by the data discussed here, whereas unequivocal examples of Neoproterozoic oceanic plateaux in the ANS have yet to be identified.

## 4. Conclusions

New Nd isotopic data for Neoproterozoic igneous rocks along the BUSZ include strongly positive initial $\varepsilon_{Nd}$ (+3.9 to +8.5) and Nd model ages (560–830 Ma) that approximate U–Pb zircon crystallization ages. The data support previous assertions based on lithological and geochemical constraints that the majority of the Jeddah and Hijaz terranes consist of juvenile Neoproterozoic crust, at least at the present level of exposure. Similar model ages for upper crustal rocks and for lower crustal and mantle lithospheric xenoliths suggest that the entire 40-km thickness of that crust was extracted from the mantle between 550 and 870 Ma, and most of it was extracted in the interval 740–830 Ma.

Although Neoproterozoic samples from the BUSZ are isotopically juvenile, inheritance of Mesoproterozoic–Archean zircon by some volcanic units indicates that continental material was involved in some of the early crust-forming events in the ANS. Compared to most BUSZ samples, those showing pre-Neoproterozoic inheritance yield slightly lower but still strongly positive $\varepsilon_{Nd}(T)$, which suggests that their juvenile parent magmas assimilated enough older material to incorporate abundant zircon grains but not enough to dramatically affect Nd isotopic systematics.

The assimilated material is estimated to be predominantly of Mesoproterozoic age with subordinate Paleoproterozoic and minor Archean components, based on the age distribution of inherited zircon. Support for this estimate is provided by the ages of inherited zircon from other studies, by crust of Paleoproterozoic–Archean age exposed in parts of the Arabian Shield, and by Mesoproterozoic–Archean model ages for upper crustal rocks and lower crustal and lithospheric mantle xenoliths in the ANS. The extent of the "contaminated shield" is approximately one-third of the ANS, reaching from the CED in Egypt to the Ar Rayn terrane in Arabia (Fig. 2).

The source of the assimilated material in the study area is debatable. Obvious sources of Paleoproterozoic–Archean zircon are the Saharan Metacraton, the Khida terrane, and basement in Yemen. The source of the dominantly Mesoproterozoic inherited zircon is problematic, because no crust of that age is exposed in the ANS and the nearest crust of this age is located >2000 km to the south in central and eastern Africa. The mechanism of inheritance is also problematic: The rounded morphologies of many inherited grains are consistent with a sedimentary origin, whereby sediments were derived from a nearby continent, transported fluvially or by glaciers, and deposited into basins undergoing arc volcanism; however, inherited grains with euhedral morphologies, which are more indicative of in situ extraction from local basement, and the occurrence of inherited zircon in the Tharwah ophiolite are more easily explained if cryptic, pre-Neoproterozoic basement underlies the Jeddah and Hijaz terranes. The location of that basement, if it exists, beneath the intra-oceanic arc terranes in the core of the ANS implies that the shield is less juvenile than presently appreciated and may contain a significant amount of continental crust, and estimates of crust-formation rates that cite the ANS as a model for juvenile crust should consider this possibility. The increasing evidence for inheritance of very old zircon in parts of the ANS previously thought to be strictly juvenile mandates further investigation to refine the extent and genesis of the contaminated shield and the nature of the underlying crust. Our findings

indicate that Nd isotopic studies alone are inadequate for detecting the subtle influences of pre-Neoproterozoic inheritance in the "juvenile" parts of the ANS. Therefore, future efforts to this end would best be served by combining detailed Nd and Pb isotopic studies with U–Pb single-zircon geochronology employing the ion microprobe, which is ideally suited to discriminating between juvenile and inherited zircon.

## Acknowledgements

Research activities for this project were funded by generous contributions from the Saudi Geological Survey for logistical support, a grant (EAR0309799) from the National Science Foundation to Stern, a Graduate Research Fellowship from NSF (0412278) and the Japan Society for the Promotion of Science to Hargrove, and a grant (7151-02) from the Geological Society of America to Hargrove. Special thanks go to the scientific staff of SGS for all of their assistance. Hargrove wishes to acknowledge Shimane University for its contributions to his fellowship in Japan and to R. Rutford for his contribution to fieldwork. We thank the referees A. Kröner and D. Stoeser and editor R. Carlson for their insightful comments and criticism to improve this manuscript. This is UTD Geosciences contribution number 1099.

## Appendix A. Sample preparation and analytical techniques

All samples analyzed in this study were processed at the University of Texas at Dallas (UTD). Billets measuring $2\times3\times4$ cm were cut from whole-rock samples on a water saw with a diamond-coated blade to remove all visible weathered or fractured surfaces. The billets were then polished to remove any metallic residue from the saw, thoroughly rinsed in deionized water, dried, and crushed in a polished-steel mortar and pestle. The crushed samples were then separated into two aliquots, which were pulverized for 30 min in tungsten carbide (for major element determination) and ceramic alumina (for trace element determination) ball mills.

Samples were digested at UTD for Sm–Nd isotopic work using the two-step procedure outlined below, which was modified after the method of Krogh [62]. Whole-rock powders measuring $0.2500\pm5$ g were partially dissolved in distilled 28.9N HF in sealed Teflon® pressure bombs while heated in an oven for three days at 200 °C. The samples were volumetrically transferred into 25 ml PFA beakers with doubly ventilated caps and were evaporated on a hot plate at 100 °C with filtered air passed through the beakers. Residues were taken up in 5 ml of distilled 15N $HNO_3$ and again evaporated at 100 °C with aeration. Residues were taken up in 1 ml of 2.5 N distilled HCl, allowed to cool for 1 h, transferred to 2 ml PP microtubes and centrifuged for 30 min. Supernatants were then pipetted into 5 ml PFA beakers, which were sealed with screw caps for temporary storage. Precipitates were transferred back into the 25 ml PFA beakers using 18.2 $M\Omega\ cm^{-1}$ deionized water from a squirt bottle, and the solutions were evaporated to dryness with aeration on a hot plate at 100 °C. The new residues were then taken up in 2 ml of 11.6 N $HClO_4$, and the solutions slowly heated over 12 h to 270 °C on a hot plate, but without aeration to prevent complete evaporation and to drive off fluorosilicates. Once at 270 °C, the solutions were evaporated to dryness with aeration to drive off the $HClO_4$. The process of centrifuging the HCl-based solutions and attacking the precipitates with $HCLO_4$ was repeated up to three times until the centrifuge precipitates were negligible.

Neodymium was extracted from the sample solutions using standard cation exchange columns. First, the light to middle rare earth elements (REE) were separated using chromatography columns pre-filled with 200–400-mesh Bio-Rad AG 50W-X8 resin. The columns were cleaned with distilled 6N HCl and conditioned with 1 ml of distilled 2.5 N HCl. The HCl-based supernatants from the final centrifuge step (above) were added to the columns and washed with 8 ml of distilled 2.5 N HCl to drive off all but the light to middle REE. The REE were then eluted from the columns with 6 ml of distilled 6N HCl and recovered in clean PFA beakers. The beakers were placed into ventilated Pyrex® jars on a hot plate, and the solutions were evaporated to dryness with aeration at 100 °C. Second, Nd was purified using quartz columns filled with HDEHP-coated S-X8 Bio-Rad Bio-beads in a procedure modified from Richard et al. [63]. The columns were cleaned with distilled 6N HCl and conditioned with 0.1 ml of 0.145 N HCl. The residues from the previous part were taken up in 0.1 ml distilled 0.145 N HCl and added to the columns. The columns were rinsed with 5–11 ml of 0.145 N HCl (actual volume varied with concentration of different batches of ~0.145 N HCl and was determined from calibration of columns by colorimetry), and Nd was eluted with 10 ml of 0.145 N HCl and collected in 10 ml PTFE beakers. The beakers were placed into ventilated Pyrex® jars on a hot plate, and the solutions were evaporated to dryness with aeration at 100 °C.

All isotopic analyses were conducted at UTD on a Finnigan MAT 261 solid-source mass spectrometer with multiple sample capabilities and 8 Faraday cups, 6 of

which are independently adjustable. Prior to analysis, neodymium from each sample was dissolved in 1 ml of dilute $HNO_3$ and transferred onto outgassed Re filaments, as were 1 ml aliquots of the La Jolla Nd standard. Analytical runs consisted of five blocks of twenty scans each for 10 unknowns and three standards, all analyzed in the dynamic multi-collection mode. During our analyses, the La Jolla Nd standard produced a mean $^{143}Nd/^{144}Nd = 0.511843 \pm 8$ over 11 analyses, and a single analysis of the USGS standard BCR-2 produced a $^{143}Nd/^{144}Nd = 0.512613 \pm 6$. Concentrations of Sm and Nd were determined separately by ICP-MS along with other trace elements not reported here. Samples were digested and analyzed at Shimane University (SU), Japan, and at UTD, as indicated in Table 1, using a method developed at SU that was briefly described by Roser et al. [64].

## Appendix B. Supplementary data

Supplementary data associated with this article can be found, in the online version, at doi:10.1016/j.epsl.2006.10.002.

## References


[1] S.R. Taylor, S.M. McLennan, The geochemical evolution of the continental crust, Rev. Geophys. 33 (1995) 241–265.

[2] R. Armstrong, The persistent myth of crustal growth, Aust. J. Earth Sci. 38 (1991) 613–630.

[3] F.M. Gradstein, J.G. Ogg, A.G. Smith, W. Bleeker, L.J. Lourens, A new geologic time scale, with special reference to Precambrian and Neogene, Episodes 27 (2004) 83–100.

[4] A. Reymer, G. Schubert, Phanerozoic addition rates to the continental crust and crustal growth, Tectonics 3 (1984) 63–77.

[5] T.H. Dixon, M.P. Golombek, Late Precambrian crustal accretion rates in Northeast Africa and Arabia, Geology 16 (1988) 991–994.

[6] P.J. Patchett, C.G. Chase, Role of transform continental margins in major crustal growth episodes, Geology 30 (2002) 39–42.

[7] R.J. Stern, Crustal evolution in the East African Orogen: a Neodymium isotopic perspective, J. Afr. Earth Sci. 34 (2002) 109–117.

[8] K. Al-Damegh, E. Sandvol, M. Barazangi, Crustal structure of the Arabian plate: new constraints from the analysis of teleseismic receiver functions, Earth Planet. Sci. Lett. 231 (2005) 177.

[9] R.J. Durrheim, W.D. Mooney, Archean and Proterozoic crustal evolution: evidence from crustal seismology, Geology 19 (1991) 606–609.

[10] F. Henjes-Kunst, R. Altherr, A. Baumann, Evolution and composition of the lithospheric mantle underneath the western Arabian Peninsula; constraints from Sr–Nd isotope systematics of mantle xenoliths, Contrib, Mineral. Petrol. 105 (1990) 460–472.

[11] A.V. McGuire, R.J. Stern, Granulite xenoliths from western Saudi Arabia: the lower crust of the late Precambrian Arabian–Nubian Shield, Contrib. Mineral. Petrol. 114 (1993) 395–408.

[12] J. Blusztajn, S.R. Hart, N. Shimizu, A.V. McGuire, Trace-element and isotopic characteristics of spinel peridotite xenoliths from Saudi Arabia, Chem. Geol. 123 (1995) 53–65.

[13] D.B. Stoeser, V.E. Camp, Pan-African microplate accretion of the Arabian shield, Geol. Soc. Amer. Bull. 96 (1985) 817–826.

[14] P.R. Johnson, B. Woldehaimanot, Development of the Arabian–Nubian shield: perspectives on accretion and deformation in the northern East African Orogen and the assembly of Gondwana, in: M.Yoshida, S. Dasgupta, B. Windley (Eds.), Proterozoic East Gondwana: Supercontinent assembly and breakup 206, Special Publication, vol. 206, Geological Society of London, London, 2003, pp. 289–325.

[15] D.B. Stoeser, M.J. Whitehouse, J.S. Stacey, The Khida terrane — geology of Paleoproterozoic rocks in the Muhayil area, eastern Arabian Shield, Saudi Arabia, Gondwana Res. 4 (2001) 192–194.

[16] M.J. Whitehouse, B.F. Windley, M.A.O. Ba-Bttat, C.M. Fanning, D.C. Rex, Crustal evolution and terrane correlation in the eastern Arabian Shield, Yemen: geochronological constraints, J. Geol. Soc. Lond. 155 (1998) 281–295.

[17] R.J. Fleck, D.G. Hadley, Ages and strontium initial ratios of plutonic rocks in a transect of the Arabian Shield, U.S. Geological Survey Open File Report USGS-OF-03-38, 1982, p. 43.

[18] J.S. Stacey, C.E. Hedge, Geochronologic and isotopic evidence for early Proterozoic crust in the eastern Arabian Shield, Geology 12 (1984) 310–313.

[19] M.J. Whitehouse, D.B. Stoeser, J.S. Stacey, The Khida Terrane; geochronological and isotopic evidence for Paleoproterozoic and Archean crust in the eastern Arabian Shield of Saudi Arabia, Gondwana Res. 4 (2001) 200–202.

[20] M.G. Abdelsalam, J.-P. Liégeois, R.J. Stern, The Saharan metacraton, J. Afr. Earth Sci. 34 (2002) 119–136.

[21] U. Harms, D.P.F. Darbyshire, T. Denkler, M. Hengst, H. Schandelmeier, Evolution of the Neoproterozoic Delgo suture zone and crustal growth in Northern Sudan: Geochemical and radiogenic isotope constraints, Geol. Rundsch. 83 (1994) 591–603.

[22] R.J. Stern, A. Kröner, R. Bender, T. Reischmann, A.S. Dawoud, Precambrian basement around Wadi-Halfa, Sudan — a new perspective on the evolution of the East Saharan Craton, Geol. Rundsch. 83 (1994) 564–577.

[23] M. Sultan, K.R. Chamberlain, S.A. Bowring, R.E. Arvidson, H. Abuzied, B. El Kaliouby, Geochronologic and isotopic evidence for involvement of pre-Pan-African crust in the Nubian Shield, Egypt, Geology 18 (1990) 761–764.

[24] A. Kröner, W. Todt, I.M. Hussein, M. Mansour, A.A. Rashwan, Dating of late Proterozoic ophiolites in Egypt and the Sudan using the single grain zircon evaporation technique, Precambrian Res. 59 (1992) 15–32.

[25] J.S. Pallister, J.S. Stacey, L.B. Fischer, W.R. Premo, Precambrian ophiolites of Arabia; geologic settings, U–Pb geochronology, Pb-isotope characteristics, and implications for continental accretion, Precambrian Res. 38 (1988) 1–54.

[26] U.S. Hargrove, R.J. Stern, W.R. Griffin, P.R. Johnson, M.G. Abdelsalam, From island arc to craton: timescales of Neoproterozoic crustal formation and deformation in the Arabian Shield, Saudi Geological Survey Technical Report (in review).

[27] U.S. Hargrove, Crustal evolution of the Neoproterozoic Bi'r Umq suture zone, Kingdom of Saudi Arabia: Geochronological, isotopic, and geochemical constraints. Unpublished Ph.D. dissertation, The University of Texas at Dallas, 2006.

[28] K.R. Ludwig, On the treatment of Concordant Uranium-Lead Ages, Geochim. Cosmochim. Acta 62 (1998) 665.

[29] J.V. Calvez, J. Delfour, J.L. Feybesse, 2000-million-year old inherited zircons in plutonic rocks from the Al Amar region: New evidence for an Early Proterozoic basement in the eastern Arabian Shield? Saudi Arabian Deputy Ministry for Mineral Resources Open File Report BRGM-OF-05-11, 1985, p. 28.
[30] A. Kennedy, P.R. Johnson, F.H. Kattan, SHRIMP geochronology in the northern Arabian Shield, Part 1: Data acquisition, Saudi Geological Survey Open File Report SGS-OF-2004-11, 2004, p. 28.
[31] J.Y. Calvez, J. Kemp, Geochronological investigations in the Mahd adh Dhahab quadrangle, central Arabian Shield, Saudi Arabian Deputy Ministry for Mineral Resources Technical Record BRGM-TR-02-5, 1982, p. 41.
[32] D.B. Stoeser, J.S. Stacey, Evolution, U–Pb geochronology, and isotope geology of the Pan-African Nabitah orogenic belt of the Saudi Arabian Shield, in: S. El Gaby, R.O. Greiling, A. Vogel (Eds.), The Pan-African Belts of Northeast Africa and Adjacent Areas, Friedr Vieweg and Sohn, Braunschweig, 1988, pp. 227–288.
[33] R.J. Fleck, Age of diorite–granodiorite gneisses of the Jiddah–Makkah region, Kingdom of Saudi Arabia, Saudi Arabian Deputy Ministry for Mineral Resources Professional Paper PP-2, 1985, pp. 19–27.
[34] V.E. Camp, Explanatory notes to accompany the geologic map of the Umm al Birak quadrangle, Sheet 23D, Kingdom of Saudi Arabia, Ministry of Petroleum and Mineral Resources, 1986, p. 40.
[35] J.N. Aleinikoff, D.B. Stoeser, Zircon morphology and U–Pb geochronology of seven metaluminous and peralkaline post-orogenic granite complexes of the Arabian Shield, Kingdom of Saudi Arabia, Open File Report USGS-OF-06-5, 1988, p. 32.
[36] J.G. Pier, F.A. Podosek, J.F. Luhr, J.C. Brannon, J.J. Aranda-Gomez, Spinel–lherzolite-bearing Quaternary volcanic centers in San Luis Potosi, Mexico; 2, Sr and Nd isotopic systematics, J. Geophys. Res. 94 (1989) 7941–7951.
[37] D.J. DePaolo, Neodymium isotopes in the Colorado Front Range and crust-mantle evolution in the Proterozoic, Nature 291 (1981) 193–196.
[38] S.L. Goldstein, R.K. O'Nions, P.J. Hamilton, A Sm–Nd isotopic study of atmospheric dusts and particulates from major river systems, Earth Planet. Sci. Lett. 70 (1984) 221–236.
[39] A.A.M. Radain, W.S. Fyfe, R. Kerrich, Origin of peralkaline granites of Saudi Arabia, Contrib. Mineral. Petrol. 78 (1981) 358–366.
[40] D.B. Stoeser, Distribution and tectonic setting of plutonic rocks of the Arabian Shield, J. Afr. Earth Sci. 4 (1985) 21–46.
[41] S.D. Samson, P.J. Patchett, W.C. McClelland, G.E. Gehrels, Nd isotopic characterization of metamorphic rocks in the Coast Mountains, Alaskan and Canadian Cordillera; ancient crust bounded by juvenile terranes, Tectonics 10 (1991) 770–780.
[42] N.B.W. Harris, I.G. Gass, C.J. Hawkesworth, A geochemical approach to allochthonous terranes; a Pan-African case study, Philos. Trans. R. Soc. Lond. Ser. A: Math. Phys. Sci. 331 (1990) 533–548.
[43] C.F. Miller, S. Meschter McDowell, R.W. Mapes, Hot and cold granites? Implications of zircon saturation temperatures and preservation of inheritance, Geology 31 (2003) 529–532.
[44] Y. Deschamps, J.L. Lescuyer, C. Guerrot, A.A. Osman, Lower Neoproterozoic age of the Ariab volcanogenic massive sulphide mineralization, Red Sea Hills, NE Sudan, 20th Colloquium of African Geology (Orléans, France) Abstracts, 2004, p. 133.
[45] D. Avigad, K. Kolodner, M. McWilliams, H. Persing, T. Weissbrod, Origin of northern Gondwana Cambrian sandstone revealed by detrital zircon SHRIMP dating, Geology 31 (2003) 227–230.
[46] R.O. Greiling, M.M. Abdeen, A.A. Dardir, H. El Akhal, M.F. El Ramly, G.M. Kamal El Din, A.F. Osman, A.A. Rashwan, A.H.N. Rice, M.F. Sadek, A structural synthesis of the Proterozoic Arabian–Nubian Shield in Egypt, Geol. Rundsch. 83 (1994) 484–501.
[47] A.E. Shimron, Evolution of the Kid Group, Southeast Sinai Peninsula; thrusts, melanges, and implications for accretionary tectonics during the late Proterozoic of the Arabian–Nubian Shield, Geology 12 (1984) 242–247.
[48] H.J. Wust, T. Reischmann, A. Kröner, W. Todt, Conflicting Pb–Pb, Sm–Nd, and Rb–Sr systematics in late Precambrian metasediments and metavolcanics from the Eastern Desert of Egypt, Terra Cogn. 7 (1987) 333.
[49] N. Miller, M. Alene, R. Sacci, R.J. Stern, A. Kröner, Conti, G. Zuppi, Significance of the Tambien Group (Tigrai, N. Ethiopia) for Snowball Earth Events in the Arabian–Nubian Shield, Precambrian Res. 121 (2003) 263–283.
[50] M. Brasier, G. McCarron, R. Tucker, J. Leather, P. Allen, G. Shields, New U–Pb zircon dates for the Neoproterozoic Ghubrah glaciation and for the top of the Huqf Supergroup, Oman, Geology 28 (2000) 175–178.
[51] J. Leather, P.A. Allen, M.D. Brasier, A. Cozzi, Neoproterozoic snowball Earth under scrutiny; evidence from the Fiq Glaciation of Oman, Geol. Boulder 30 (2002) 891–894.
[52] M. Beyth, D. Avigad, H.U. Wetzel, A. Matthews, S.M. Berhe, Crustal exhumation and indications for snowball Earth in the East African Orogen: north Ethiopia and east Eritrea, Precambrian Res. 123 (2003) 187.
[53] H.E. Frimmel, U.S. Klötzli, P.R. Siegfried, New Pb–Pb single zircon age constraints on the timing of Neoproterozoic glaciation and continental break-up in Namibia, J. Geol. 104 (1996) 459–469.
[54] M.G. Abdelsalam, R.J. Stern, Tectonic evolution of the Nakasib suture, Red Sea Hills, Sudan: evidence for a late Precambrian Wilson cycle, J. Geol. Soc. Lond. 150 (1993) 393–404.
[55] P.R. Johnson, M. Abdelsalam, R.J. Stern, The Bi'r Umq–Nakasib shear zone: Geology and structure of a Neoproterozoic suture in the northern East African Orogen, Saudi Arabia and Sudan, Technical Report SGS-TR-2002-1, 2002, p. 33.
[56] P.R. Johnson, M.G. Abdelsalam, R.J. Stern, The Bi'r Umq–Nakasib suture zone in the Arabian–Nubian Shield; a key to understanding crustal growth in the East African Orogen, Gondwana Res. 6 (2003) 523–530.
[57] J.R. Lancelot, D. Bosch, A Pan African age for the HP–HT granulite gneisses of Zabargad Island; implications for the early stages of the Red Sea rifting, Earth Planet. Sci. Lett. 107 (1991) 539–549.
[58] D.B. Stoeser, C.D. Frost, Nd, Pb, Sr, and O isotopic characterization of Saudi Arabian Shield terranes, Chem. Geol. (2006) 43.
[59] A. Reymer, G. Schubert, Rapid growth of some major segments of continental crust, Geology 14 (1986) 299–302.
[60] M. Stein, S.L. Goldstein, From plume head to continental lithosphere in the Arabian–Nubian Shield, Nature 382 (1996) 773–778.
[61] M. Stein, A.W. Hofmann, Mantle plumes and episodic crustal growth, Nature 372 (1994) 63–68.
[62] T.E. Krogh, A low-contamination method for hydrothermal decomposition of zircon and extraction of U and Pb for isotopic age determinations, Geochim. Cosmochim. Acta 37 (1973) 485–494.
[63] P. Richard, N. Shimizu, C.J. Allegre, (super 143) Nd/ (super 146) Nd, a natural tracer; an application to oceanic basalts, Earth Planet. Sci. Lett. 31 (1976) 269–278.
[64] B. Roser, J.-I. Kimura, K. Hisatomi, Whole-rock elemental abundances in sandstones and mudrocks from the Tanabe Group,

Kii Peninsula, Japan, Geoscience Report, vol. 19, Shimane University, 2000, pp. 101–112.
[65] R.A. Agar, J.B. Stacey, M.J. Whitehouse, Evolution of the southern Afif terrane—a geochronologic study, Saudi Arabian Deputy Ministry for Mineral Resource Open File Report DGMR-OF-10-15, 1992, p. 41.
[66] B.F. Windley, M.J. Whitehouse, M.A.O. Ba-Bttat, Early Precambrian gneiss terranes and Pan-African island arcs in Yemen; crustal accretion of the eastern Arabian Shield, Geology 24 (1996) 131–134.
[67] M.J. Whitehouse, B.F. Windley, D.B. Stoeser, S. Al-Khirbash, M.A.O. Ba-Bttat, A. Haider, Precambrian basement character of Yemen and correlations with Saudi Arabia and Somalia, Precambrian Res. 105 (2001) 357.
[68] J.S. Stacey, R.A. Agar, U–Pb isotopic evidence for the accretion of a continental micro-plate in the Zalm region of the Saudi Arabian Shield, J. Geol. Soc. Lond. 142 (1985) 1189–1203.
[69] E. Hegner, J.S. Pallister, Pb, Sr, and Nd isotopic characteristics of Tertiary Red Sea Rift volcanics from the central Saudi Arabian coastal plain, J. Geophys. Res. 94 (1989) 7749–7755.
[70] D.B. Stoeser, M.J. Whitehouse, R.A. Agar, J.S. Stacey, Pan-African accretion and continental terranes of the Arabian Shield, Eos 72 (1991) 299.
[71] L. Loizenbauer, E. Wallbrecher, H. Fritz, P. Neumayr, A.A. Khudeir, U. Kloetzli, Structural Geology, single zircon ages and fluid inclusion studies of the Meatiq metamorphic core complex: implications for Neoproterozoic tectonics in the Eastern Desert of Egypt, Precambrian Res. 110 (2001) 357–383.
[72] H.J. Duyverman, N.B.W. Harris, C.J. Hawkesworth, Crustal accretion in the Pan African; Nd and Sr isotope evidence from the Arabian Shield, Earth Planet. Sci. Lett. 59 (1982) 315–326.